This scenario is verified by the behavior of the distinct part of the van Hove correlation function:

$$G_d(r,\tau) = \frac{1}{N}\left\langle \sum_{i\neq j}^{N}\sum \delta[r + r_j(0) - r_i(\tau)] \right\rangle \quad (4)$$

This function is proportional to the probability of finding a particle $i \neq j$ in a region dr around r at time τ, provided that a particle j was at the origin at $\tau = 0$. In Fig. 5, we plotted $g_d(r,\tau) = G_d(r,\tau)/\rho$, where ρ is the in-plane number density, for the system with $\phi = 0.52$ at several times. Even at times where diffusive behavior is observed (compare with Fig. 3), there is a considerably smaller probability of finding a particle in the region $0 < r < 1$ relative to finding it elsewhere. The same trend was observed in the other systems with $\phi \leq 0.52$ (*27*). This result demonstrates that the onset of the diffusive regime reflects the behavior of the more mobile fraction of particles: Diffusive behavior is apparent even though the systems bear significant memory of their local structure.

We have shown that a system in which only excluded volume interactions operate exhibits dynamical heterogeneities. These heterogeneities manifest themselves in a non-Gaussian self-part of the van Hove correlation function and influence the onset of apparent long-time diffusion.

References and Notes

1. P. G. Debenedetti, *Metastable Liquids* (Princeton Univ. Press, Princeton, NJ, 1996).
2. C. A. Angell, *Science* **267**, 1924 (1995).
3. H. Sillescu, *J. Non-Cryst. Solids* **243**, 81 (1999).
4. M. T. Cicerone and M. D. Ediger, *J. Chem. Phys.* **103**, 5684 (1996).
5. K. Schmidt-Rohr and H. W. Spiess, *Phys. Rev. Lett.* **66**, 3020 (1991).
6. M. Hurley and P. Harrowell, *Phys. Rev. E* **52**, 1694 (1995).
7. W. Kob *et al.*, *Phys. Rev. Lett.* **79**, 2827 (1997).
8. B. Doliwa and A. Heuer, *Phys. Rev. Lett.* **80**, 4915 (1998).
9. A. Kasper, E. Bartch, H. Sillescu, *Langmuir* **14**, 5004 (1998).
10. T. C. Mortensen and W. van Megen, in *Slow Dynamics in Complex Systems*, M. Tokuyama and I. Oppenheim, Eds. (American Institute of Physics, Woodbury, NY, 1998), p. 3.
11. W. Poon, P. N. Pusey, H. N. W. Lekkerkerker, *Phys. World* (April), 27 (1996).
12. W. van Megen and S. M. Underwood, *Nature* **362**, 616 (1993).
13. A. van Blaaderen, G. Bosma, Z. Dogic, C. Pathmamanoharan, W. K. Kegel, in preparation.
14. A. van Blaaderen and A. Vrij, *Langmuir* **8**, 2921 (1992).
15. L. Antl *et al.*, *Colloid Surf.* **17**, 67 (1986).
16. C. Pathmamanoharan, C. Slob, H. N. W. Lekkerkerker, *Colloid Polymer Sci.* **267**, 448 (1989).
17. W. Schaertl and H. Sillescu, *J. Stat. Phys.* **77**, 1007 (1994).
18. J. C. Crocker and D. G. Grier, *J. Colloid Interface Sci.* **179**, 298 (1996).
19. J. Bongers *et al.*, *J. Chem. Phys.* **108**, 9937 (1998).
20. A. van Blaaderen and P. Wiltzius, *Science* **270**, 1177 (1995).
21. P. N. Pusey and W. van Megen, *Nature* **320**, 340 (1986).
22. T. M. Truskett *et al.*, *Phys. Rev. E* **58**, 3083 (1998).
23. J. P. Hansen and I. R. McDonald, *Theory of Simple Liquids* (Academic Press, London, 1986).
24. B. R. A. Nijboer and A. Rahman, *Physica* **32**, 415 (1966).
25. J. K. G. Dhont, in *An Introduction to Dynamics of Colloids*, D. Möbius and R. Miller, Eds. (Elsevier, Amsterdam, 1996), pp. 327–329.
26. M. Fuchs, W. Götze, M. R. Mayr, *Phys. Rev. E* **58**, 3384 (1998).
27. W. K. Kegel and A. van Blaaderen, data not shown.
28. We thank G. Bosma, Z. Dogic, and C. Pathmamanoharan for their contribution in preparing the core-shell particles; J. Hoogenboom for computing $g(r)$ in three dimensions; H. Lekkerkerker for many discussions during initialization of this work and for continuous interest; and G. Koenderink and D. Frenkel for comments on the manuscript. W.K.K. thanks P. Harrowell for enlightening discussions and correspondence. Supported by the Royal Dutch Academy of Arts and Sciences (W.K.K.) and by FOM, which is part of the Netherlands Organization for Scientific Research.

16 August 1999; accepted 15 November 1999

Formation of Cyclic Water Hexamer in Liquid Helium: The Smallest Piece of Ice

K. Nauta and R. E. Miller*

The cyclic water hexamer, a higher energy isomer than the cage structure previously characterized in the gas phase, was formed in liquid helium droplets and studied with infrared spectroscopy. This isomer is formed selectively as a result of unique cluster growth processes in liquid helium. The experimental results indicate that the cyclic hexamer is formed by insertion of water molecules into smaller preformed cyclic complexes and that the rapid quenching provided by the liquid helium inhibits its rearrangement to the more stable cage structure.

The study of neutral water clusters holds considerable promise for obtaining a molecular level description of the properties of bulk water. Through the investigation of progressively larger clusters, it is becoming possible to systematically probe the various n-body terms in the corresponding intermolecular potential. Intense experimental (*1–6*) and theoretical (*7–10*) work has focused on the detailed characterization of the water dimer, trimer, tetramer, and larger clusters. The structural landscape associated with the larger clusters is quite rich, and theoretical studies have revealed many different local minima on the associated potential energy surfaces that correspond to a range of structural isomers. Many of these isomers are reminiscent of transient structures that appear in liquid water and the tetrahedral network of ice, which suggests that their study can provide insights into the bulk properties of water.

Despite this rich landscape, the current experimental studies of small water clusters have revealed only a single (the most stable) isomer for each cluster size, which greatly limits the configuration space that can be explored in this way. In the present study, we use superfluid liquid helium as a growth medium to access a different portion of the structural landscape and in particular report the experimental observation of the cyclic water hexamer. The importance of this observation can be appreciated by noting that the cyclic hexamer is one of the prominent morphologies found in computer simulations of liquid water and is the structural motif for ice I_h (*11*, *12*). The ab initio structure of the cyclic water hexamer (*9*, *13*, *14*) is shown in Fig. 1, along with the cage isomer characterized previously by Saykally and coworkers (*1*, *2*).

The apparatus used in the present study has been discussed in some detail previously (*15*). Helium droplets are formed by expanding ultrapure helium gas from a pressure of ~60 bar through a 5-μm-diameter nozzle that is cooled to 19 to 22 K with a closed-cycle helium refrigerator. These droplets pass through the pick-up chamber, which was maintained at a variable water pressure to control the number of molecules they capture. Cluster formation within the droplet is ensured if more than one water molecule is captured because the interactions between molecules are far stronger than those between water and helium.

Before discussing the experimental results, it is important to consider how cluster growth in liquid helium differs from homogeneous nucleation in a free jet expansion and why the two methods might be expected to give rise to different structures. In a free jet, nucleation occurs early in the expansion, and the clusters subsequently cool by two-body collisions. This relatively slow cooling (compared with that in liquid helium) facilitates the annealing of clusters

---

Department of Chemistry, University of North Carolina, Chapel Hill, NC 27599, USA.

*To whom correspondence should be addressed. E-mail: remiller@unc.edu

into their lowest energy configuration. In contrast, helium droplets capture the water molecules (according to Poisson statistics) with an average time between capture events on the order of tens of microseconds. This time scale is extremely long, even with respect to the slow relaxation of intramolecular vibrations in gas-phase complexes (*16*), and so we can assume that the water molecules are completely cooled between capture events. Thus, a water trimer is formed when a cold water monomer [0.38 K (*17*)] combines with a similarly cold dimer, and so forth for larger clusters. In a previous study on HCN (*18*), we showed that this mechanism led to the exclusive formation of linear chains, where each molecule is captured, cooled, and oriented by their mutual interaction at large separations. The rapid quenching provided by the liquid helium removes the condensation energy that is released upon cluster formation, so that if there are barriers on the intermolecular potential between the approach geometry and the global minimum on the surface, the system becomes trapped in a local minimum. Once a certain structural motif is established, major rearrangements will be difficult, again because thermal energy is extremely limited in the liquid helium environment.

Although water dimers and trimers have been observed previously in liquid helium (*19*), the structures that have been observed to date are the same as in the gas phase. In particular, the trimer has been shown to form the most stable, cyclic structure. For these two clusters, the spectra we report here are in good agreement with the previous study. The open, chainlike trimer is also known to be a minimum on the ab initio surface (*20*). Nevertheless, the intensities of the O–H stretches associated with this isomer are weaker than the hydrogen-bonded mode of the cyclic trimer, which makes it more difficult to detect.

We now consider what will happen when a fourth water molecule approaches a preformed cyclic trimer. There is some evidence from the study of Buck and co-workers (*21*) on methanol clusters in helium that, once the cyclic trimer is formed and cooled, insertion of the fourth molecule into the ring is inhibited by the lack of energy needed to open the ring. The result would be the formation of a tetramer structure corresponding to a cyclic trimer with the fourth molecule hydrogen bonded to the outside. The goal of the present study is to investigate whether the growth of water clusters larger than the trimer in liquid helium might lead to a different structural motif than that obtained in gas phase.

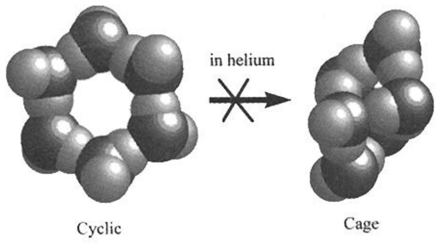

Fig. 1. Cyclic and cage isomers of the water hexamer, based on the ab initio calculations of Xantheas (*25*).

The infrared spectrum obtained for the O–H stretches of water clusters formed in liquid helium is shown in Fig. 2 and compared with that of the corresponding complexes formed in a free jet expansion. As noted above, the dimer and trimer bands are essentially the same in the two cases, with the exception that the bands are sharper in the liquid helium spectrum because of the correspondingly lower temperature. The vibrational frequency shifts resulting from the interactions with the helium are negligible on this scale and make the assignment of the dimer and trimer straightforward. However, we also observe transitions in coincidence with the gas-phase tetramer and pentamer bands at 3416 and 3360 cm^{-1}, respectively (*22*). The implication is that water molecules have managed to insert into the trimer ring in the low-energy environment of the helium, in sharp contrast with the results on methanol (*21*). Apparently, there is a low barrier pathway corresponding to insertion of a water molecule into a trimer or a tetramer ring. This result is quite surprising given that there are a number of minima on the tetramer surface that correspond to a trimer ring with the fourth molecule bound to the outside (*23*, *24*). Although some theoretical work has been reported on the transition states between the various local minima on these water cluster surfaces (*24*), the specific problem at hand has not been addressed, and the present results underscore the need for further theoretical work in this area. A possible explanation for the difference between the water and methanol systems is that, in the former, ring insertion is facilitated by tunneling of the hydrogen atoms through the associated barriers. In contrast, ring insertion may be inhibited in methanol because it involves more heavy atom motion.

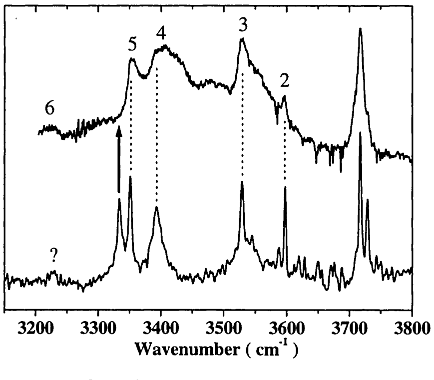

Fig. 2. Infrared spectra of the O–H stretching vibrations of water clusters formed in the gas phase (top curve) and in liquid helium droplets (bottom curve). The numbers correspond to the cluster size. The question mark indicates a weak band in the helium droplet spectrum that is at the frequency corresponding to the caged hexamer structure. This peak could be due to a small amount of caged hexamer that manages to rearrange in helium or may be associated with even larger clusters.

The most interesting feature in the helium spectrum, which is noticeably absent from the gas-phase spectrum, is the additional peak to the red of the pentamer. We examined the dependence of the relative intensities of these peaks on the water pressure in the pick-up region to confirm that this additional band is associated with a cluster larger than the pentamer. For the cage form of the water hexamer (*1*, *2*) (Fig. 1), the most intense O–H vibrational band is shifted much further to the red (labeled 6 in Fig. 2) than the new band observed here. As shown below, there is considerable evidence supporting the assignment of this new band to the cyclic isomer of the water hexamer.

The most compelling support for this assignment comes from comparing the frequency shifts for all of these cyclic complexes with the corresponding ab initio calculations of Xantheas (*25*), as shown in Fig. 3. The frequency shifts vary smoothly with cluster size, and the new cyclic hexamer peak is precisely where it is expected based on a smooth extrapolation from the smaller rings. This behavior is reproduced essentially quantitatively by the ab initio calculations. Better agreement than this is probably not expected given that the theoretical values are

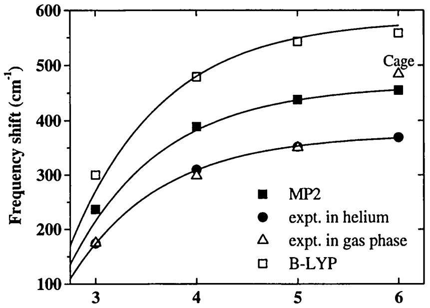

Fig. 3. A plot of the experimental and calculated (*25*) vibrational redshifts for cyclic water clusters, from the trimer to the hexamer. The shifts are measured in both cases relative to the average of the symmetric and asymmetric O–H stretches of the monomer, to be consistent with (*25*). In the gas phase, the hexamer forms a cage, and the associated frequency shift is large with respect to those of the cyclic structures. As expected from the spectra in Fig. 2, the frequency shifts are essentially the same for the gas and liquid helium data for clusters up to the pentamer. The solid curve is a fit to the experimental helium data points and is provided to guide the eye. The curves through the ab initio MP2 and B-LYP points were generated by simply multiplying this fitted curve by 1.24 and 1.55, respectively, to give the best fit to these calculated values. The new band observed in the helium droplet spectrum appears at the frequency one would expect from the ab initio calculations for the cyclic hexamer (scaled to the experimental shifts for the other cyclic clusters).

based on harmonic frequency calculations. Although these cyclic clusters all have multiple O–H vibrational bands, the most intense ones for each cluster size (the ring stretches) are close in frequency and thus merge into a single band, which is particularly intense. Indeed, ab initio calculations show that the intensities of the O–H modes associated with less symmetric structures, in which the molecules are inequivalent, are much smaller than for the cyclic structures (*26*). Analogous effects were observed in the case of the linear chains of HCN (*27*), where the most redshifted C–H stretches have the highest intensity. The application of a large electric field has no influence on this band, which further supports the cyclic structure. In contrast with the polar chains of HCN reported previously (*28*), for which an electric field markedly sharpens and intensifies the spectrum, the equilibrium geometry for the cyclic water hexamer is nonpolar and no such effect is expected. The cyclic tetramer is also nonpolar, and although the cyclic trimer and pentamer have polar equilibrium structures, vibrational averaging yields an effective dipole moment of zero (*29*).

Having established that the water molecules insert into a preexisting hydrogen-bonded ring of smaller size, the continuation of this growth pattern naturally leads to the formation of a cyclic hexamer. The path between this hexamer and the cage will involve a great deal of hydrogen bond rearrangement, which we expect will be difficult in liquid helium (see Fig. 1). Apparently, there is not enough energy available to the system to reach the three-dimensional cage. Several other local minima lie lower in energy than the cyclic hexamer (*26*). Thus, we have not simply formed the next higher energy isomer of the hexamer but rather have used this growth process to steer the system kinetically to this specific structural isomer.

Despite considerable effort, we found no evidence for the cyclic heptamer in the helium spectra. At the present time, we are unsure whether this means that the cyclic heptamer is not stabilized by the helium or if the frequency shift between this species and the cyclic hexamer is simply too small to permit us to resolve the corresponding peaks. We note that there is a weak band further to the red (indicated by the question mark in Fig. 1), which could be due to either a small amount of cage hexamer that has managed to rearrange or the heptamer in a cage form. Further ab initio calculations on both the cyclic and cage forms of the heptamer will be helpful in determining what happens with the larger water clusters grown in helium.

These experiments show that growth in liquid helium can provide access to different structures than those obtained from gas-phase nucleation, allowing us to explore at least some of the rich structural landscape that has been identified by theoretical calculations. The cyclic water hexamer is the smallest possible ice-like cluster, and its detailed study should provide important insights into the properties of bulk ice. Molecular dynamics studies show that this cyclic motif is also important in liquid water. The present study suggests a class of experiments that, when combined with the corresponding theoretical calculations, could shed light on this interesting hydrogen bond ring insertion process. Because a chainlike trimer has also been shown to be a local minimum on the corresponding surface (*20*), we are hopeful that with further improvements to the sensitivity of the apparatus, water chains might also be observed.

References and Notes

1. K. Liu *et al.*, *Nature* **381**, 501 (1996).
2. K. Liu, M. G. Brown, R. J. Saykally, *J. Phys. Chem. A* **101**, 8995 (1997).
3. N. Pugliano and R. J. Saykally, *Science* **257**, 1937 (1992).
4. J. D. Cruzan *et al.*, *Science* **271**, 59 (1996).
5. U. Buck, I. Ettischer, M. Melzer, V. Buch, J. Sadlej, *Phys. Rev. Lett.* **80**, 2578 (1998), and references therein.
6. J. Brudermann *et al.*, *J. Chem. Phys.* **110**, 10649 (1999), and references therein.
7. C. J. Tsai and K. D. Jordan, *Chem. Phys. Lett.* **213**, 181 (1993).
8. J. Kim, D. Majumdar, H. M. Lee, K. S. Kim, *J. Chem. Phys.* **110**, 9128 (1999), and references therein.
9. S. S. Xantheas and T. H. Dunning Jr., *J. Chem. Phys.* **99**, 8774 (1993).
10. M. R. Viant *et al.*, *J. Chem. Phys.* **110**, 4369 (1999).
11. A. C. Belch and S. A. Rice, *J. Chem. Phys.* **86**, 5676 (1987).
12. R. J. Speedy, J. D. Madura, W. L. Jorgensen, *J. Phys. Chem.* **91**, 909 (1987).
13. B. J. Mhin, S. Kim, H. S. Kim, C. W. Yoon, K. S. Kim, *Chem. Phys. Lett.* **176**, 41 (1991).
14. J. M. Pedulla, K. Kim, K. D. Jordan, *Chem. Phys. Lett.* **291**, 78 (1998).
15. K. Nauta and R. E. Miller, *J. Chem. Phys.* **111**, 3426 (1999).
16. R. E. Miller, *Science* **240**, 447 (1988).
17. M. Hartmann, R. E. Miller, J. P. Toennies, A. F. Vilesov, *Phys. Rev. Lett.* **75**, 1566 (1995).
18. F. Remacle and R. D. Levine, *Int. J. Quantum Chem.* **67**, 85 (1998).
19. R. Frochtenicht, M. Kaloudis, M. Koch, F. Huisken, *J. Chem. Phys.* **105**, 6128 (1996).
20. S. S. Xantheas, *Philos. Mag. B* **73**, 107 (1996).
21. M. Behrens, R. Frochtenicht, M. Hartmann, S. Jorg-Gerald, U. Buck, *J. Chem. Phys.* **111**, 2436 (1999).
22. F. Huisken, M. Kaloudis, A. Kulcke, *J. Chem. Phys.* **104**, 17 (1996).
23. D. J. Wales and T. R. Walsh, *J. Chem. Phys.* **106**, 7193 (1997).
24. C. J. Tsai and K. D. Jordan, *J. Phys. Chem.* **97**, 11227 (1993).
25. S. S. Xantheas, *J. Chem. Phys* **102**, 4505 (1995); private communication.
26. J. Kim and K. S. Kim, *J. Chem. Phys.* **109**, 5886 (1998).
27. M. Kofranek, A. Karpfen, H. Lischka, *Chem. Phys.* **113**, 53 (1987).
28. K. Nauta and R. E. Miller, *Science* **283**, 1895 (1999).
29. M. G. Brown, F. N. Keutsch, R. J. Saykally, *J. Chem. Phys.* **109**, 9645 (1998).
30. We are grateful to L. Oudejans for help with the gas-phase water cluster spectra and S. Xantheas for several helpful discussions and for providing us with a more extensive set of MP2 calculations than is currently available in the literature. This work was supported by NSF (CHE-97-10026). We also acknowledge the donors of the Petroleum Research Fund, administered by the American Chemical Society, for partial support of this research.

30 September 1999; accepted 11 November 1999

Distal Initiation and Active Propagation of Action Potentials in Interneuron Dendrites

Marco Martina,[1] Imre Vida,[2] Peter Jonas[1]*

Fast and reliable activation of inhibitory interneurons is critical for the stability of cortical neuronal networks. Active conductances in dendrites may facilitate interneuron activation, but direct experimental evidence was unavailable. Patch-clamp recordings from dendrites of hippocampal oriens-alveus interneurons revealed high densities of voltage-gated sodium and potassium ion channels. Simultaneous recordings from dendrites and somata suggested that action potential initiation occurs preferentially in the axon with long threshold stimuli, but can be shifted to somatodendritic sites when brief stimuli are applied. After initiation, action potentials propagate over the somatodendritic domain with constant amplitude, high velocity, and reliability, even during high-frequency trains.

γ-Aminobutyric acid (GABA)–containing interneurons control the activity of cortical neuronal networks (*1*). Interneurons mediate feedback and feedforward inhibition (*2*), set the threshold for initiation of axonal Na^+ action potentials and dendritic Ca^{2+} spikes in principal neurons (*3*), and participate in the generation of oscillatory activity (*4*). In many circuits, interneurons operate as coincidence detectors or relays that are activated with very short delay by a small number of principal neurons (*5*). The mech-

---

[1] Physiologisches Institut der Universität Freiburg, [2] Anatomisches Institut der Universität Freiburg, D-79104 Freiburg, Germany.

*To whom correspondence should be addressed. E-mail: jonasp@ruf.uni-freiburg.de